

# Inosculation of Blood Vessels Allows Early Perfusion and Vitality of Bladder Grafts—Implications for Bioengineered Bladder Wall

Stephanie L. Osborn, PhD,<sup>1,2</sup> Michelle So, MA,<sup>1,2</sup> Shannon Hambro,<sup>1,2</sup>  
Jan A. Nolta, PhD,<sup>2,3</sup> and Eric A. Kurzrock, MD<sup>1,2</sup>

Bioengineered bladder tissue is needed for patients with neurogenic bladder disease as well as for cancer. Current technologies in bladder tissue engineering have been hampered by an inability to efficiently initiate blood supply to the graft, ultimately leading to complications that include graft contraction, ischemia, and perforation. To date, the biological mechanisms of vascularization on transplant have not been suitably investigated for urologic tissues. To better understand the mechanisms of neovascularization on bladder wall transplant, a chimeric mouse model was generated such that angiogenesis and vasculogenesis could be independently assessed *in vivo*. Green fluorescence protein (GFP) transgenic mice received bone marrow transplants from  $\beta$ -galactosidase (LacZ) transgenic animals and then subsequent bladder wall transplants from wild-type donor mice. Before euthanization, the aorta was infused with fluorescent microbeads (fluorospheres) to identify perfused vessels. The contributions of GFP (angiogenesis) and LacZ (vasculogenesis) to the formation of CD31-expressing blood vessels within the wild-type graft were evaluated by immunohistochemistry at different time points and locations within the graft (proximal, middle, and distal) to provide a spatiotemporal analysis of neovascularization. The GFP index, a measure of angiogenic host ingrowth, was significantly higher at proximal versus mid or distal regions in animals 2–16 weeks post-transplant. However, GFP index did not increase over time in any area. Within 7 days post-transplant, perfusion of primarily wild-type, donor blood vessels in the most distal areas of the graft was observed by intraluminal fluorospheres. In addition, chimeric host-donor (GFP-wild type) blood vessels were evident in proximal areas. The contribution of vasculogenesis to vascularization of the graft was limited, as LacZ cells were not specifically associated with the endothelial cells of blood vessels, but rather found primarily in areas of inflammation. The data suggest that angiogenesis of host blood vessels into the proximal region leads to inosculation between host and donor vessels and subsequent perfusion of the graft via pre-existing graft vessels within the first week after transplant. As such, the engineering of graft blood vessels and the promotion of inosculation might prevent graft contraction, thereby potentiating the use of bioengineered bladder tissue for transplantation.

## Introduction

**T**HERE IS A NEED for bioengineered bladder, particularly among pediatric patients with spina bifida and spinal cord injury. An ideal substitute for the bladder wall would be bioengineered tissue containing the patient's own cells. Urologic tissue engineering research has focused on developing substrates (synthetic and decellularized scaffolds) that support muscle and urothelial, but not specifically vascular, regeneration. Bladder augmentation with bioengineered tissue or acellular scaffolds has been highly successful in small animal models. On the other hand, results have not

been consistent in large animal models or humans due to graft contraction.<sup>1–3</sup> Seminal work by Atala *et al.* in 2006 demonstrated that augmentation of the human bladder with cell-seeded constructs was feasible.<sup>1</sup> However, a follow-up phase II study in 10 children showed no improvement in bladder capacity, where 4 patients had urine leakage due to perforation or nonhealing.<sup>4</sup> The contraction and failure of large grafts is likely multifactorial, although ischemia is considered the principle component.

Using a syngeneic, male-to-female bladder transplant model, we previously described cellular interactions between the host bladder and donor tissue by tracking the Y

<sup>1</sup>Department of Urology, University of California, Davis School of Medicine, Sacramento, California.

<sup>2</sup>Stem Cell Program, Institute for Regenerative Cures, University of California, Davis Medical Center, Sacramento, California.

<sup>3</sup>Department of Internal Medicine, University of California, Davis School of Medicine, Sacramento, California.

chromosome in transplanted cells till 16 months after surgery.<sup>5</sup> At 16 months, graft muscle demonstrated persistence of male cells. On the other hand, male graft urothelium was partially replaced by female host cells. Results from our study and others have shown that bone marrow stem cells have a role in urothelial and muscle regeneration.<sup>5-7</sup> While there has been significant focus on vascularization for other tissues, vascular architecture and endothelialization have not been suitably investigated for bladder wall engineering.

Unlike solid organ transplantation, which entails major vessel anastomoses, the transplantation of tissue without major vessels depends on rapid angiogenesis and inosculation. A process called plasmatic imbibition, in which the graft absorbs plasma, initially nourishes free grafts, such as skin and possibly bladder. The next step is capillary inosculation, when host vessels grow into the graft and anastomose with donor vessels. In human-to-mouse skin graft models, this usually occurs within 2-5 days and chimeric mouse/human vessels are observed.<sup>8-10</sup> Finally, neovascularization occurs with the growth of host vessels deep into the graft. A skin graft is quite different than the bladder since the surface area between host and donor is vast, allowing extensive imbibition and inosculation.

New vessel formation is not exclusively via angiogenesis, which is defined by the formation of new blood vessels from pre-existing ones. Another important mechanism, vasculogenesis, occurs when endothelial progenitor cells (EPCs) migrate and differentiate in response to local cues to form new endothelial cells and blood vessels. Vasculogenesis is not limited to embryogenesis. In adults, EPCs increase in

response to ischemia and contribute to neovascularization after trauma and transplantation.<sup>6,11</sup>

In this study, the mechanisms of neovascularization after bladder wall transplantation were evaluated to determine the roles of angiogenesis, vasculogenesis, and inosculation. Our results suggest that pre-existing vessels within a bladder graft might facilitate early perfusion, thereby promoting graft survival and function.

**Materials and Methods**

*Animals*

Female green fluorescence protein (GFP) transgenic mice [C57Bl/6TG(UBC-GFP)30Scha/J], male  $\beta$ -galactosidase (LacZ) transgenic mice [B6.12957-GJ(ROSA)26Sor/J], and C57Bl6 wild-type mice (males and females) were obtained from Jackson Laboratories and maintained at University of California, Davis Medical Center (UCDMC) in accordance with institutional standards of care and Institutional Animal Care and Use Committee (IACUC)-approved protocols. The experimental procedures described next are illustrated in Figure 1A.

*Bone marrow transplant*

Female GFP transgenic mice were subjected to total body irradiation at 1050 CyG. LacZ male mice were euthanized; bone marrow was collected from femurs, tibias, and spine; and  $10 \times 10^6$  cells per animal were injected into the tail vein of lethally irradiated GFP female mice. Negative control animals

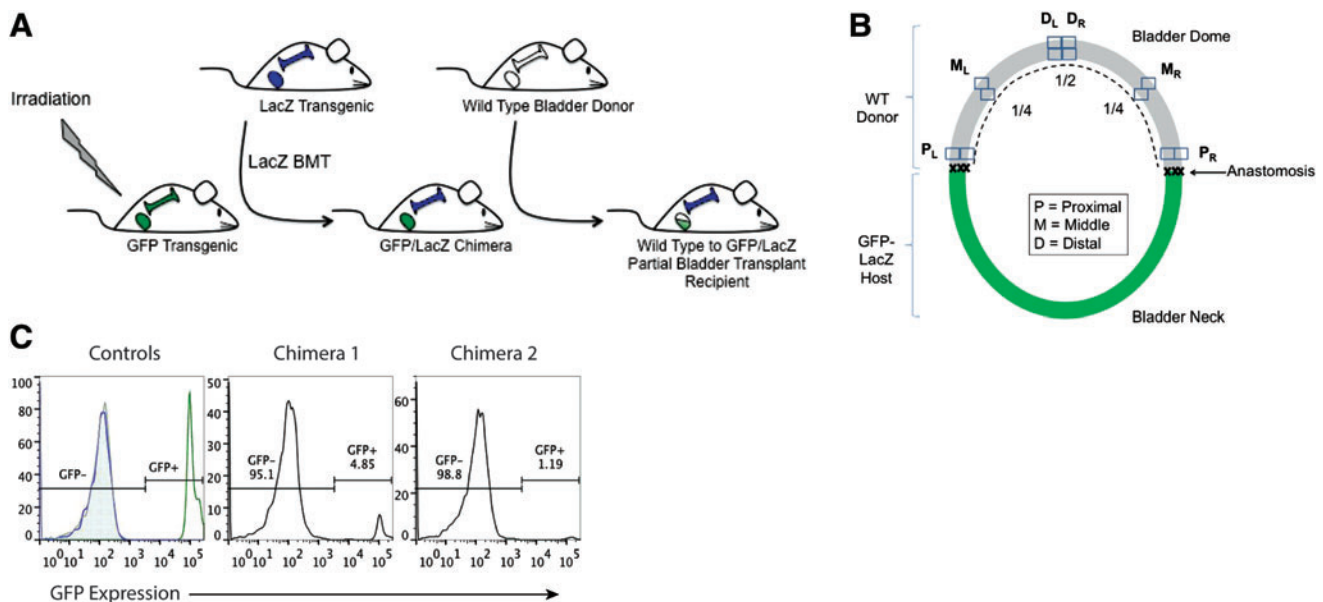


**FIG. 1.** Generation and analysis of green fluorescence protein (GFP)/LacZ chimeric mice for bladder wall transplant. (A) Female GFP transgenic mice were irradiated and received bone marrow transplants (BMTs) from LacZ transgenic mice. The resulting GFP/LacZ chimeras were then host to a bladder wall transplant from a wild-type male donor, such that angiogenesis could be evaluated via ingrowth from the GFP host and vasculogenesis could be evaluated via *de novo* growth from the LacZ<sup>-</sup>-expressing bone marrow. (B) Illustration of GFP/LacZ bladder post-wild-type bladder wall transplant. Proximal, middle, and distal regions relative to the anastomosis were analyzed to provide a spatial analysis of angiogenesis and vasculogenesis over time. (C) Flow cytometry analysis of GFP expression in the peripheral blood of control and chimeric animals, as a measure of LacZ engraftment post-BMT. Controls are wild type (shaded gray histogram), LacZ (blue line histogram), and GFP transgenic (green line histogram). Color images available online at [www.liebertpub.com/tea](http://www.liebertpub.com/tea)

received irradiation but no bone marrow transplant (BMT) and, subsequently, died within 40 days postirradiation. At least 1 month post-BMT, tail vein blood was collected and assessed for LacZ engraftment via flow cytometry, as evidenced by loss of GFP expression (BD Fortessa LSRII; FlowJo, TreeStar, Inc.). GFP/LacZ chimeric animals were used as hosts for bladder wall transplants at 5–8 months post-BMT.

#### Bladder wall transplant

Before surgery, GFP/LacZ chimeric females were given prophylactic Baytril (enrofloxacin) at 2 mg/kg i.p. once daily for 2 days. At surgery, chimeric females were anesthetized by isoflurane, shaved, Betadine-scrubbed, and given preoperative i.p. Metacam (meloxicam; 2 mg/kg) and Baytril (5 mg/kg) for analgesia and prophylaxis, respectively. The skin and fascia were opened with a small midline incision, and the abdominal muscles were separated. The bladder was brought external to the body cavity and exposed. The dome of the bladder was incised<sup>12,13</sup> and a donor graft from the dome of a syngeneic, wild-type male mouse bladder, ~5 mm in diameter, was sewn on with a running 8-0 Vicryl suture (Ethicon). The urethra was catheterized with a 24-gauge angiocatheter (BD Biosciences), and the bladder was inflated to verify a watertight anastomosis. Leaks were fixed with interrupted 8-0 sutures. Single-knot, superficial 6-0 prolene sutures were placed in the host portion of the bladder, just beneath the anastomosis to serve as long-term markers of the host/graft border. Animals were given postoperative care that included daily injections of Metacam and Baytril for 3 days.

#### Tissue preparation and immunohistochemistry

At various time points postsurgery (1, 2, 4, 8, and 16 weeks), transplant recipients were euthanized, catheterized with a 24 g angiocatheter, and their bladders were distended with 100  $\mu$ L of phosphate-buffered saline (PBS). The urethra was ligated with the angiocatheter intact, and the bladder was dissected from the host animal and incubated in 1:1 OCT:PBS solution at 4°C for 30 min. The intravesical PBS was replaced with OCT and the bladder was frozen, bisected longitudinally, and embedded in OCT. Bladders were cryosectioned into 6  $\mu$ m-thick tissue sections. Standard H&E staining for frozen sections was performed to observe tissue histology. To assess angiogenesis, slides containing consecutive tissue sections were briefly fixed with 4% paraformaldehyde (PFA) and immunofluorescently stained for CD31 (559761; BD Pharmingen), GFP (ab290; Abcam), and DAPI. To assess vasculogenesis, slides were fixed in glutaraldehyde/PFA and stained for LacZ, as per kit instructions (Mirus), followed by CD31 (559761; BD Pharmingen) staining using a rabbit anti-rat biotin secondary antibody (Life Technologies) and DAB chromagen detection (Vector Laboratories).

#### Fluorosphere perfusion

Transplant recipients (11 total) were injected intraperitoneally with 300  $\mu$ L of 50  $\mu$ g/mL nitroglycerin and then euthanized 10 min later. The right atrium was incised, and the blood was removed by flushing 30 mL PBS into the left ventricle using a 30 g needle. The descending abdominal

aorta was catheterized with a 24 g angiocatheter, and 2 mL of Dark Red 0.2  $\mu$ m Fluorospheres<sup>®</sup> microbeads (660/680 nm, diluted 1:10; Molecular Probes) were perfused with steady, gentle pressure. Bladders were harvested and preserved as already described.

#### Data analysis and statistics

For angiogenesis contribution (GFP host endothelium in the wild-type graft), three consecutive tissue sections of each bladder were analyzed. Initially, a 4 $\times$  image of the entire graft and anastomotic area was assembled using the stitch function on the Bioevo Fluorescence Microscope (BZ-9000; Keyence). From that 4 $\times$  map, proximal, middle, and distal areas were identified relative to the anastomotic border on both sides of the bladder. The anastomosis was identified based on sutures, and the proximal area was set at ~200  $\mu$ m into the graft from the anastomosis on each side. The distal area was set at half the distance between proximal areas, and the middle regions were set at the midpoint between proximal and distal areas (Fig. 1B). Each area was imaged for GFP, CD31, and DAPI as serial 60 $\times$  images taken progressively from the lumen to the outer serosa of the bladder wall. Postacquisition image analysis was performed using ImageJ (NIH, Wayne Rasbald). Vessels were identified by CD31 (red) staining and manually selected using the marking tools. Each 60 $\times$  image was calibrated such that pixel density is a measure of area (1 pixel = 0.17761  $\mu$ m), and CD31<sup>+</sup> area was acquired using the Analyze Particles tool. Microvessel density (MVD) is the ratio of the CD31 area to that of the entire tissue area ( $\mu$ m<sup>2</sup>). Subsequently, CD31<sup>+</sup> vessels were analyzed for their relative expression of GFP. A positive GFP<sup>+</sup> signal was determined using various biologic and experimental controls and set with the Thresholding tool. The area of the GFP signal (specifically within the CD31<sup>+</sup> regions of interest) was calculated using the Analyze Particles tool and the contribution of GFP to MVD is reported as GFP index = GFP (pixels) / CD31 (pixels) for the proximal, middle, and distal areas of each transplant bladder. Tissue sections stained for LacZ and CD31 were analyzed subjectively, such that areas of LacZ were documented.

For statistical analysis of the data, the GFP index and vascularity were compared between regions and time points post-transplant using linear mixed-effects models. These models included fixed effects for region, time point, and their interaction, and random effects for mouse and slide (tissue section). GFP index data were log transformed before analysis, with a small constant added to the data before transformation to avoid taking the log of 0. Vascularity data were log transformed. Analyses were conducted using the statistical software environment R, version 3.1.1 (R Core Team, 2014). Linear mixed-effects modeling was conducted using the R package lme4, version 1.1–7.<sup>14</sup> *p*-Values were adjusted for multiple testing (within each table) using the single-step method of Hothorn *et al.*<sup>15</sup>

## Results

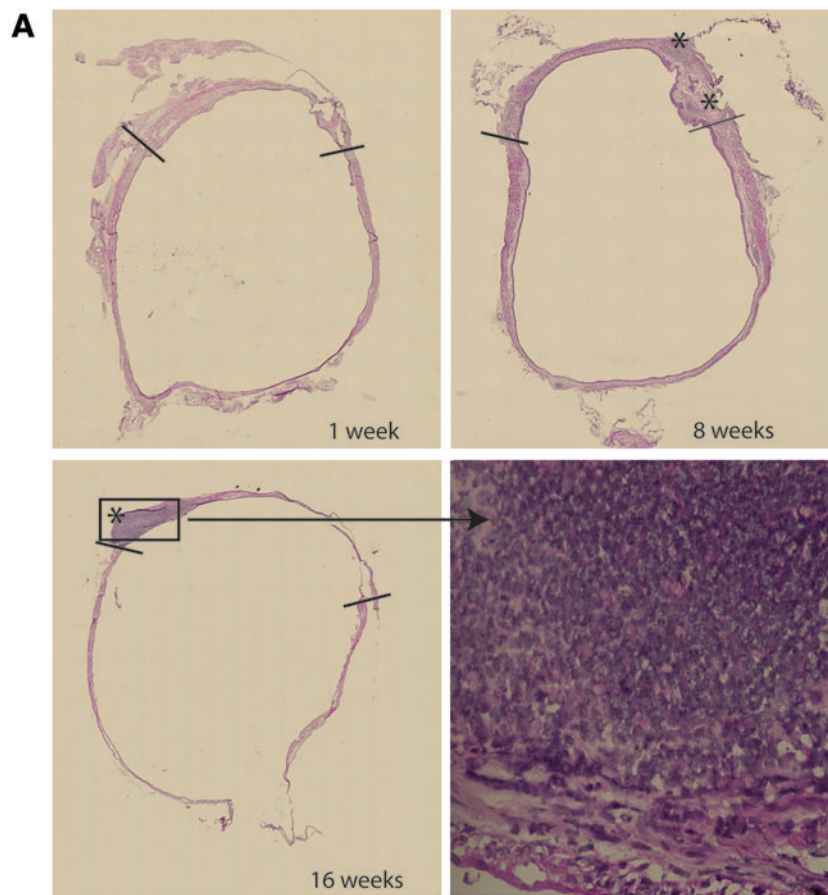
To assess the contribution of angiogenesis and vasculogenesis to graft survival on bladder wall transplant, we generated a chimeric animal model that would allow for differential analysis of these two distinct processes, both spatially and temporally, within the same animal (Fig. 1A).

TABLE 1. SUMMARY OF SURVIVAL AND ANALYSES STATISTICS

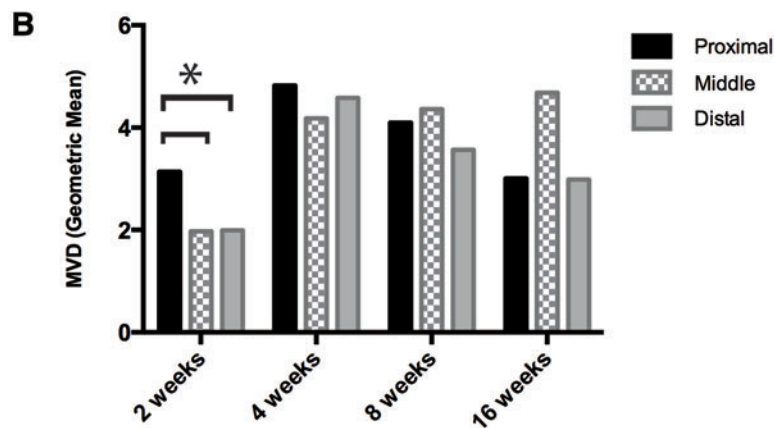
Bladder transplants	Survived/ rate (%)	Time-points (week)	Histologically analyzed	Fluorosphere perfused (analyzed)
65	31/48	1	3	3 (3)
		2	3	1 (1)
		4	3	3 (1)
		8	3	2 (2)
		16	3	2 (2)

Using a ubiquitous GFP transgenic mouse as the host, BMTs were performed using bone marrow from a syngeneic LacZ transgenic mouse. At 1 month post-BMT, GFP mice were tested for reconstitution of their bone marrow with LacZ. Peripheral blood samples were analyzed for their expression of GFP via flow cytometry (Fig. 1C). In comparison to negative (wild type, LacZ) and positive GFP animal controls, LacZ BMT recipients showed loss of GFP expression, down to less than 5%, indicating a successful transplant.

At 5–8 months post-BMT, GFP/LacZ chimeric mice then received wild-type mouse bladder wall transplants. Angiogenesis is represented by the ingrowth of GFP<sup>+</sup> host blood vessels into the wild-type graft, while vasculogenesis is



**FIG. 2.** Histological analyses of grafts. (A) H&E staining of 1, 8, and 16 week bladders post-transplant (10× magnification; *stitch*), including a close-up of an inflammatory area, densely packed with nuclei (60× magnification). (B) Microvessel density (MVD; geometric mean) in P, M, and D areas from animals at 2, 4, 8, and 16 weeks post-transplant. Asterisk (\*) indicates statistical significance. Color images available online at [www.liebertpub.com/tea](http://www.liebertpub.com/tea)





represented by *de novo* formation of blood vessels from LacZ<sup>+</sup> bone marrow-derived cells.

We performed 65 bladder transplants on GFP/LacZ chimeric mice, with an overall survival rate of 48%. Grafts from mice that were sick or died prematurely to their designated collection time point were not analyzed. Because graft failure is multi-faceted (technical, biological, physiological) and because our intent was to investigate the mechanism of successful blood supply initiation on bladder wall transplant, we also limited our analyses to animals with healthy grafts, that is, grafts that were free of contraction (greater than 2 mm in length) and free of significant edema. Fifteen of 31 grafts from 1 to 16 weeks post-transplant met these inclusion criteria ( $n=3$  for each time point) (Table 1).

Bladder sections were analyzed histologically via standard H&E staining (Fig. 2A). Anastomotic areas were identified by the presence of sutures, as well as tissue histology. Areas of inflammation were present primarily in anastomotic and proximal areas and were evident till 16 weeks post-transplant. This is in congruence with our previous work in rats, where inflammation persisted till 6 months post-transplant.<sup>5</sup>

The microvessel density (MVD) was calculated for each graft at each of the proximal, middle, and distal areas as a ratio of the area of CD31<sup>+</sup> to total tissue area. The MVD was subjected to pairwise main-effect comparisons between regions and was adjusted for time points. Vascularity was found to be significantly higher in the proximal

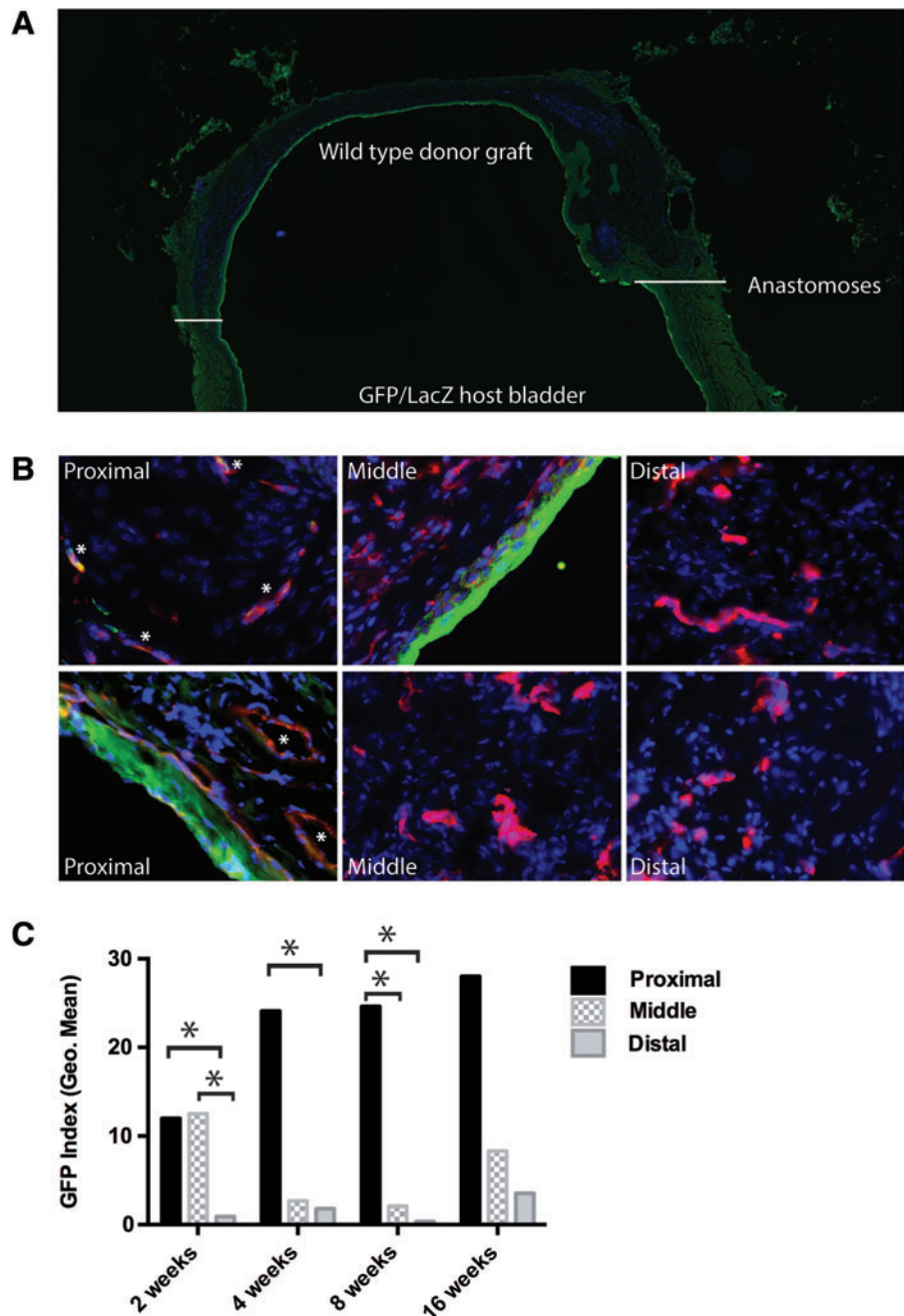


**FIG. 3.** Angiogenesis occurs in proximal regions of the graft. (A) Eight-week post-transplant bladder stained for GFP (green), CD31 (red), and nuclei (DAPI, blue); 10 $\times$  magnification. White lines identify the anastomotic regions. (B) Representative images of proximal, middle, and distal areas from 8-week graft; 60 $\times$  magnification. (C) Graphical representation of the GFP index (geometric mean) at each of the three regions from animals at 2, 4, 8, and 16 weeks post-transplant. Statistically significant differences are indicated by asterisks (\*). When adjusted for time point, the GFP index of P>D ( $p<0.001$ ) and P>M ( $p=0.002$ ) in any given animal at any time point. Color images available online at [www.liebertpub.com/tea](http://www.liebertpub.com/tea)

regions than in both the distal and middle regions ( $p=0.031$ ) at 2 weeks post-transplant (Fig. 2B). However, this difference was small and not visually obvious. There was no statistical difference in MVD in any region at 4, 8, or 16 weeks post-transplant.

*Host ingrowth and contribution to neovascularization*

In accordance with our previously published results with rat bladder transplants, donor muscle remained intact, while GFP urothelial cells from the host bladder gradually replaced donor wild-type urothelium (Fig. 3A). GFP host serosal tissue, from either ingrowth and/or adhesion, was also present on the outside of the transplanted bladder graft. Ingrowth of these tissues may contribute additional mechanisms of neovascularization and although important, we were specifically interested in the process of neovascularization resulting from the anastomosis of host and donor bladder tissue. Thus, blood vessels within the serosa were excluded from subsequent analysis. Although it does not typically contain blood vessels, the urothelium was excluded from analysis for technical reasons, as an extremely bright GFP signal from host urothelial ingrowth impeded on neighboring fields.

The ingrowth of GFP<sup>+</sup> host vessels (ratio of GFP<sup>+</sup> to CD31<sup>+</sup> blood vessels) into the wild-type bladder graft represents angiogenesis and was calculated as the GFP index, as described in Figure 1C and the Materials and Methods section. The GFP index was calculated for 12 animals, 2–16 weeks post-transplant. One-week bladders were too difficult to accurately analyze, especially in the proximal areas, due to the early state of repair and presence of infiltrating cells.

Figure 2 depicts a bladder graft at 8 weeks post-transplant and representative pictures from proximal, middle, and distal areas (Fig. 3A, B). The geometric mean of the GFP index for each time point and region is plotted in Figure 3C, and statistical differences between regions within individual time points are indicated. On adjusting for time points, pairwise main-effect comparisons of the GFP index between P, M, and D regions show that the GFP index is significantly higher in the proximal region compared with both the distal ( $p<0.001$ ) and middle ( $p=0.002$ ) regions in a given animal. This suggests that angiogenesis does occur, but it is spatially limited to the proximal regions. In contrast, the GFP index did not differ significantly between 2, 4, 8, and 16 weeks, either when P, M, and D areas were tested in aggregate or when they were tested separately. Thus, there was no temporal change in the amount of angiogenesis after 2 weeks post-transplant. This suggests that angiogenesis and inosculation were completed within the first 2 weeks post-transplant.

To ascertain the presence and establish the origin of functional vessels within the graft, we perfused the aorta of 11 mice with fluorescent microspheres and analyzed their presence within blood vessels of the bladder at various time points. Seven grafts that met the inclusion criteria, as described earlier, were analyzed for perfusion at 1, 8, and 16 weeks (Table 1). At 1 week post-transplant, fluorospheres are evident in both GFP<sup>+</sup> (host) and GFP<sup>-</sup> (wild-type donor) CD31<sup>+</sup> vessels in the proximal region. In contrast, fluorospheres are observed in the distal regions of the graft, but primarily within GFP<sup>-</sup> negative, wild-type vessels (Fig. 4A–C). This observation is consistent at 8 and 16 weeks post-transplant. We analyzed 20 distal fields in animals at 1,

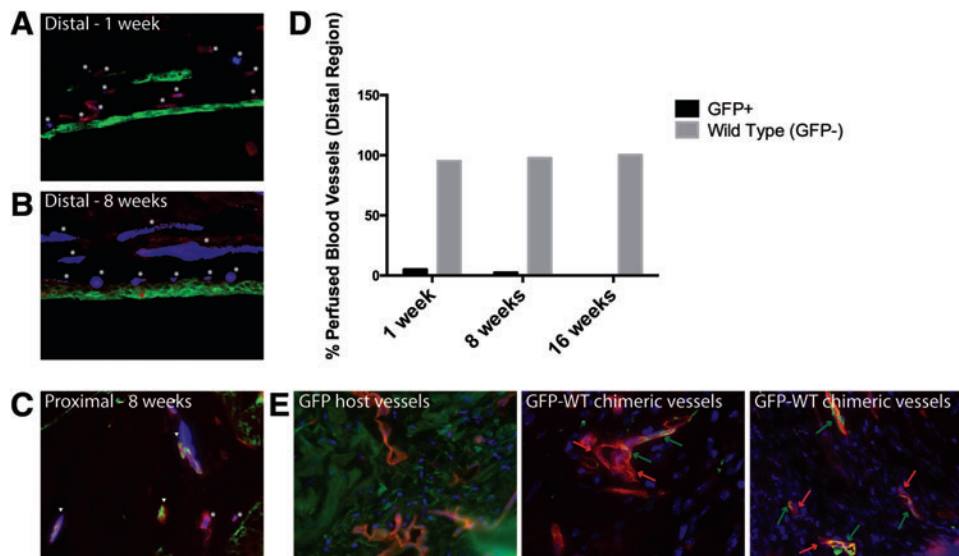


**FIG. 4.** Perfusion in distal regions of bladder grafts occurs primarily through wild-type donor blood vessels. (A, B) Representative distal fields from 1- to 8-week animals show the origin of perfused vessels. Perfused microspheres (blue) are found in CD31<sup>+</sup> (red) vessels, which are either GFP<sup>+</sup> (host, green; arrow heads) or GFP<sup>-</sup> (wild-type donor; asterisk); 60× magnification. (C) Representative proximal field from 8-week animals shows both perfused GFP<sup>+</sup> and GFP<sup>-</sup> blood vessels; 60× magnification. (D) Graphical representations of the relative percentage of GFP<sup>+</sup> (host) versus wild-type (GFP<sup>-</sup>, donor) blood vessels in distal areas from 1-, 8-, and 16-week animals. (E) Proximal areas from 2-week transplant bladders were stained for CD31 (red), GFP (green), and nuclei (blue, DAPI) and analyzed for host (GFP<sup>+</sup>) or donor (wild type, GFP<sup>-</sup>) cells within blood vessels. Possible GFP-WT chimeric blood vessels are indicated via red and green arrows, pointing to areas within a vessel that are GFP<sup>-</sup> (donor, red only) and GFP<sup>+</sup> (host, yellow-orange), respectively. GFP host vessels are shown as a positive control for GFP<sup>+</sup> blood vessels (yellow-orange); 60× magnification. Color images available online at [www.liebertpub.com/tea](http://www.liebertpub.com/tea)

8, and 16 weeks post-transplant, counting at least 40 blood vessels per time point, to calculate the relative percentages of wild type (GFP<sup>-</sup>, donor) and GFP<sup>+</sup> (host) blood vessels with fluorescent microspheres (Fig. 4D). At 1 week, only 5% of the perfused vessels at the distal region of the graft are GFP<sup>+</sup> (host), while 95% are GFP<sup>-</sup> (WT; wild type donor). At 8 weeks, the ratio is 2.4% GFP:97.6% WT and at 16 weeks, the ratio is 0% GFP:100% WT. Thus, the vast majority of functional vessels in the distal area of the bladder graft belong to the donor; they are not vessels formed from angiogenic ingrowth from the host bladder.

We hypothesized that donor blood vessels are functional as a result of anastomosis between host and donor vessels in the proximal region, resulting in vessel inosculature and supply of blood to the graft. As evidence of this inosculature, GFP<sup>-</sup> wild-type chimeric blood vessels are evident in

the proximal regions of bladder grafts at 2 weeks post-transplant (Fig. 4E). In contrast, chimeric vessels were not observed within distal graft regions.

#### Bone marrow contribution to neovascularization

Vasculogenesis is the process of *de novo* vessel formation from bone marrow-derived progenitor cells. Because GFP hosts received LacZ BMTs, LacZ-derived blood vessels would provide evidence of vasculogenesis post-transplant.

LacZ-expressing cells were observed to be scattered in various areas of bladder grafts. As bone marrow cells have been shown to be involved in urothelial regeneration, it was not surprising that LacZ expression was noted in the urothelium of the graft portion. However, LacZ<sup>+</sup> cells were particularly evident in anastomotic and proximal areas,

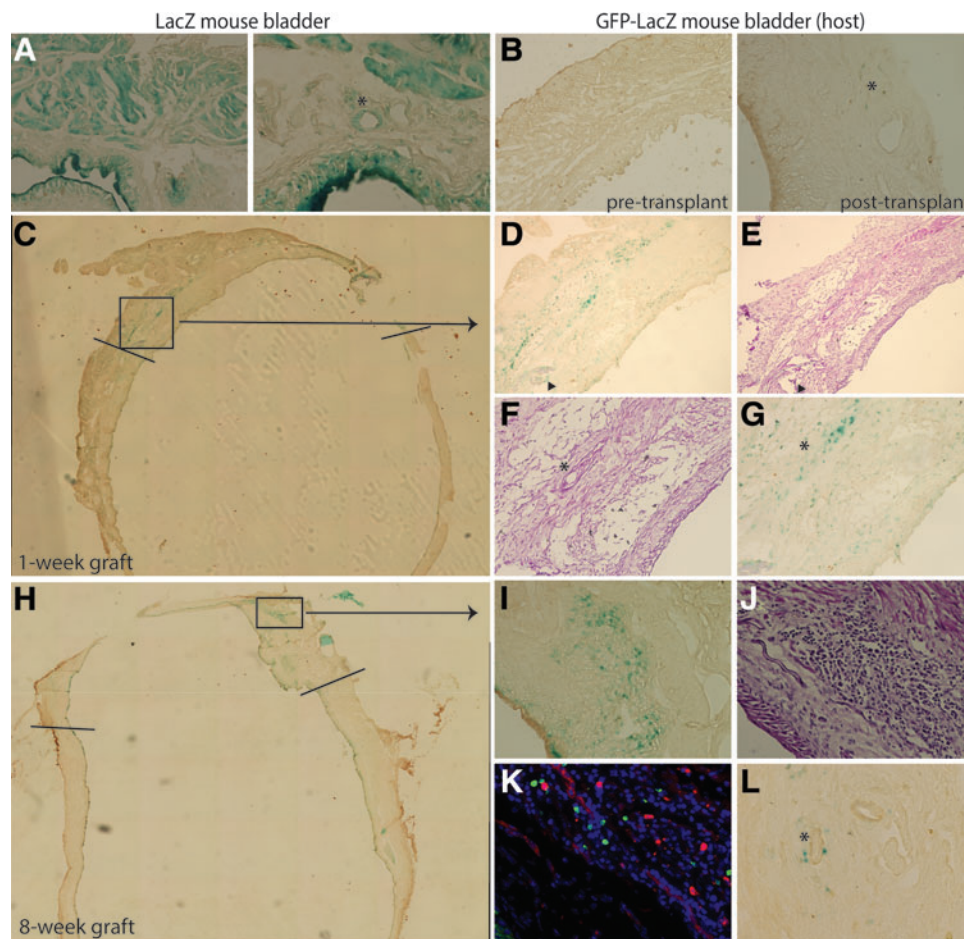


**FIG. 5.** Limited vasculogenesis in an intact bladder wall transplant. Immunohistochemical analysis of bladder tissues from control animals (A, B) or bladder transplant recipients (C–L). (A) LacZ is highly expressed in LacZ transgenic tissues. Asterisk (\*) denotes LacZ<sup>+</sup> vessel. LacZ as green, CD31 as brown; 20× (left) and 60× (right) magnifications. (B) LacZ is not expressed in GFP/LacZ chimeric host bladder tissue pretransplant (left; 20× magnification) and only minimally after transplant (right; 40× magnification). Asterisk (\*) denotes LacZ<sup>+</sup> cells. (C–G) One-week post-transplant bladder. (C) LacZ/CD31 staining of the graft; 10× magnification. Lines demarcate the anastomoses. (D) LacZ staining correlates with inflammatory infiltrates, as seen by H&E (E); 10× magnification. Arrowheads indicate sutures in the anastomotic region. (F, G) LacZ staining is found within vessels, but not as a part of the vessels; H&E (F) and LacZ/CD31 (G); 40× magnification. (H–L) Eight-week post-transplant bladder. (H) LacZ staining of the graft; 10× magnification. Lines demarcate the anastomoses. LacZ staining in (I) correlates with inflammatory infiltrates, as seen by H&E in (J); 40× magnification. (K) Immunofluorescent stain demonstrates a small percentage of GFP<sup>+</sup> infiltrates in the same inflammatory area captured in (I, J) (GFP, green; CD31, red; nuclei-DAPI, blue); 60× magnification. (L) LacZ<sup>+</sup> cells observed around a vessel; 40× magnification. Color images available online at [www.liebertpub.com/tea](http://www.liebertpub.com/tea)



including those that histologically resembled inflammation via H&E staining (Fig. 5D, E, I, J) and the amount of LacZ staining generally decreased over time post-transplant (Fig. 5C vs. 5H). Small pools of GFP-expressing cells, not associated with vessels, were observed in these same areas of inflammation (Fig. 5K). As the bone marrow of chimeric mice still had approximately 5% GFP cells post-BMT, the presence of both GFP and LacZ cells (at a ratio of 5%:95%, respectively) in these inflammatory areas likely represents infiltrating immune cells. Importantly, LacZ staining was not specifically associated with CD31<sup>+</sup> blood vessels. In some cases, LacZ<sup>+</sup> cells were observed in and/or around blood vessels, but could not be reliably identified as endothelial cells (Fig. 5F, G, L). Since CD31 and LacZ failed to co-express, the role for vasculogenesis appears limited in full-thickness bladder graft transplants.

**Discussion**

Augmentation of the bladder is often necessary for the treatment of children with dysfunctional bladders due to spinal dysraphism and spinal cord injury.<sup>16</sup> Current surgical techniques utilize ileum, colon, or stomach as a substitute for bladder tissue. Unfortunately, gastrointestinal segments have inherent absorptive and secretory properties that lead to recurrent urinary infection, stone formation, and electrolyte imbalance.<sup>17-19</sup> The most concerning issue is the increased incidence of adenocarcinoma. Most tumors present more than 10 years after augmentation, so as the life expectancy of children with spina bifida increases, a major concern is the latency of these tumors.

Despite significant advances in cell culture techniques and development of advanced synthetic substrates, vascularization has become the most critical and pressing component of urologic tissue engineering, bridling human application. Although it seems intuitive that bladder wall transplants would follow similar mechanistic principles as skin grafts, the physical properties are actually opposite.

Free skin grafts or substitutes contact the host across a large surface area for prompt imbibition and inosculation, nourishing a relatively thin graft. The ratio of contact surface area to graft thickness can be more than 100:1. On the other hand, bladder grafts have a very, very small area of anastomotic area relative to the length of the graft with an anastomotic area to graft length ratio of less than 1:100. We did not know whether the small number of vessels available at the anastomosis would sufficiently allow imbibition and inosculation. Animal and human trials have shown that placement of the omentum on the graft is critical to prevent contraction. We purposely did not mobilize the omentum such that survival of the graft depended on the host-donor anastomosis.

Angiogenesis is limited to several tenths of micrometers per day,<sup>20</sup> and complete neo-vascularization of the studied grafts (2 mm and greater) would require weeks. At early time points, there was minimal ingrowth of host (GFP) vessels beyond the proximal portion of the grafts. Although angiogenesis could have been slower in this model, it does not explain the near absence of GFP<sup>+</sup> host vessels in the distal regions of viable grafts at 16 weeks. In conjunction with the fluorosphere perfusion of middle and distal wild-type donor vessels by 7 days and evidence of GFP-wild-type

chimeric vessels in the proximal regions, these results demonstrate early inosculation (host-to-donor anastomoses) with perfusion via the wild-type donor vessels.

In this chimeric mouse model, LacZ expression was evident at early time points due to the high degree of inflammation, particularly near the anastomoses. Endothelium, pericytes, and/or white blood cells could have been the source. Our results demonstrate that bone marrow-derived cells are involved with the early inflammatory phase, as well as with regeneration of the graft urothelium. However, as LacZ and CD31 failed to co-localize, there was no significant presence of EPC-derived endothelium or vasculogenesis. Kajbafzadeh *et al.* found evidence of vasculogenesis (CD34<sup>+</sup> cells) in a rat acellular bladder augment model.<sup>21</sup> Without pre-existing vessels in a graft, the bone marrow is highly likely to be involved with vessel formation. In the present model, with donor vessels present, vasculogenesis was minimal, yet this does not disprove the involvement of bone marrow-derived cells via paracrine or other modulatory actions.

As the overall amount of angiogenesis (GFP index) did not increase over time or beyond proximal regions and the contribution of vasculogenesis was not significant, we theorize that the relatively quick (less than 7 days) inosculation of host and donor vessels in proximal regions is physiologically sufficient to keep grafts vital in the long term. As such, inosculation and a lack of ischemic signals obviated significant neovascularization or ingrowth of host vessels beyond the proximal area.

Although the limited number of vessels at the anastomosis were capable of imbibition and inosculation, the process is not likely very efficient and may contribute to the low animal survival and significant contraction rates (both about 50%) in the mouse transplant model. The availability of syngeneic GFP and LacZ transgenic (or similar) rats limited our use of a larger animal model for the current studies. In our rat bladder transplant studies, survival was greater than 90%.<sup>5</sup> However, a 50% rate of survival for mice postbladder transplant is consistent with other studies and is likely due to the technical challenge of creating a watertight anastomosis.<sup>12</sup> In addition, mice less than 5 months post-BMT exhibited only a 30% survival rate on bladder transplant. Thus, to achieve nearly 50% survival rate, we chose to use animals between 5 and 8 months post-BMT for these studies. While this older animal age and 3-month surgical window may introduce some bias in outcome, successful surgery and recovery was also paramount to vascularization and tissue regeneration.

We speculate that the process of inosculation at the anastomosis provides the fastest initiation of blood supply, compared with complete neovascularization, but is still limited in a large graft. Thus, in the clinical setting, the use of omentum is critical for enhancing blood supply to the graft. Bioengineering of blood vessels has been investigated for nonbladder tissues, while cells (mesenchymal stem cells, endothelial cells) and growth factors have been used to enhance vascular growth into bladder grafts.<sup>22-28</sup> The results of this study suggest that pre-existing vessels in bioengineered grafts might facilitate early perfusion and enhance graft regeneration and function in the long term. As such, the engineering of graft blood vessels and the promotion of inosculation between host and donor vessels,



either endogenous or engineered, might promote graft success, thereby potentiating the use of bioengineered bladder tissue for transplantation.

### Acknowledgments

This work was supported by a grant from Shriners Hospitals for Children to E.A.K. (85600-NCA). The authors thank Dr. Blythe Durbin-Johnson for statistical analysis and Katie Howard for assistance with data analysis. This project was also supported in part by the University of California Davis Flow Cytometry Shared Resource Laboratory, with funding from the NCI P30 CA0933730, NIH NCRR C06-RR12088, S10 RR12964, and S10 RR 026825 grants and with technical assistance from Bridget McLaughlin and Jonathan Van Dyke.

### Disclosure Statement

No competing financial interests exist.

### References

- Atala, A., Bauer, S.B., Soker, S., Yoo, J.J., and Retik, A.B. Tissue-engineered autologous bladders for patients needing cystoplasty. *Lancet* **367**, 1241, 2006.
- Roth, C.C., Mondalek, F.G., Kibar, Y., Ashley, R.A., Bell, C.H., Califano, J.A., Madhally, S.V., Frimberger, D., Lin, H.K., and Kropp, B.P. Bladder regeneration in a canine model using hyaluronic acid-poly(lactic-co-glycolic-acid) nanoparticle modified porcine small intestinal submucosa. *BJU Int* **108**, 148, 2011.
- Yoo, J.J., Meng, J., Oberpenning, F., and Atala, A. Bladder augmentation using allogenic bladder submucosa seeded with cells. *Urology* **51**, 221, 1998.
- Joseph, D.B., Borer, J.G., De Filippo, R.E., Hodges, S.J., and McLorie, G.A. Autologous cell seeded biodegradable scaffold for augmentation cystoplasty: phase II study in children and adolescents with spina bifida. *J Urol* **191**, 1389, 2014.
- Tanaka, S.T., Thangappan, R., Eandi, J.A., Leung, K.N., and Kurzrock, E.A. Bladder wall transplantation—long-term survival of cells: implications for bioengineering and clinical application. *Tissue Eng Part A* **16**, 2121, 2010.
- Asahara, T., Masuda, H., Takahashi, T., Kalka, C., Pastore, C., Silver, M., Kearne, M., Magner, M., and Isner, J.M. Bone marrow origin of endothelial progenitor cells responsible for postnatal vasculogenesis in physiological and pathological neovascularization. *Circ Res* **85**, 221, 1999.
- Tanaka, S.T., Martinez-Ferrer, M., Makari, J.H., Wills, M.L., Thomas, J.C., Adams, M.C., Brock, J.W., 3rd, Pope, J.C., 4th, and Bhowmick, N.A. Recruitment of bone marrow derived cells to the bladder after bladder outlet obstruction. *J Urol* **182**, 1769, 2009.
- Young, D.M., Greulich, K.M., and Weier, H.G. Species-specific in situ hybridization with fluorochrome-labeled DNA probes to study vascularization of human skin grafts on athymic mice. *J Burn Care Rehabil* **17**, 305, 1996.
- Nor, J.E., Peters, M.C., Christensen, J.B., Sutorik, M.M., Linn, S., Khan, M.K., Addison, C.L., Mooney, D.J., and Polverini, P.J. Engineering and characterization of functional human microvessels in immunodeficient mice. *Lab Invest* **81**, 453, 2001.
- Tremblay, P.L., Hudon, V., Berthod, F., Germain, L., and Auger, F.A. Inoculation of tissue-engineered capillaries with the host's vasculature in a reconstructed skin transplanted on mice. *Am J Transplant* **5**, 1002, 2005.
- Asahara, T., and Kawamoto, A. Endothelial progenitor cells for postnatal vasculogenesis. *Am J Physiol Cell Physiol* **287**, C572, 2004.
- Mauney, J.R., Cannon, G.M., Lovett, M.L., Gong, E.M., Di Vizio, D., Gomez, P., 3rd, Kaplan, D.L., Adam, R.M., and Estrada, C.R., Jr. Evaluation of gel spun silk-based biomaterials in a murine model of bladder augmentation. *Biomaterials* **32**, 808, 2011.
- Tu, D.D., Seth, A., Gil, E.S., Kaplan, D.L., Mauney, J.R., and Estrada, C.R., Jr. Evaluation of biomaterials for bladder augmentation using cystometric analyses in various rodent models. *J Vis Exp pii*: 3981, 2012.
- Bates, D., Maechler, M., Bolker, B.M., and Walker, S. lme4: linear mixed-effects models using Eigen and S4. Available at: <http://arXiv:1406.5823>, accessed June 23, 2014.
- Hothorn, T., Bretz, F., and Westfall, P. Simultaneous inference in general parametric models. *Biom J* **50**, 346, 2008.
- Kurzrock, E.A., and Polse, S. Renal deterioration in myelodysplastic children: urodynamic evaluation and clinical correlates. *J Urol* **159**, 1657, 1998.
- Kurzrock, E.A., Baskin, L.S., and Kogan, B.A. Gastrocystoplasty: long-term followup. *J Urol* **160**, 2182, 1998.
- McDougal, W.S. Metabolic complications of urinary intestinal diversion. *J Urol* **147**, 1199, 1992.
- Nguyen, H.T., and Kurzrock, E.A. The effect of enterocystoplasty on skeletal development in children. In: Stone, A.R., ed. *Urinary Diversion*. 2nd edition. London: Martin Dunitz, 2004.
- Clark, E.R.C., and Clark, E.L. Microscopic observations on the growth of blood capillaries in the living mammal. *Am J Anat* **64**, 251, 1939.
- Kajbafzadeh, A.M., Payabvash, S., Salmasi, A.H., Sadeghi, Z., Elmi, A., Vejdani, K., Tavangar, S.M., Tajik, P., and Mahjoub, F. Time-dependent neovascularogenesis and regeneration of different bladder wall components in the bladder acellular matrix graft in rats. *J Surg Res* **139**, 189, 2007.
- Baranski, J.D., Chaturvedi, R.R., Stevens, K.R., Eyckmans, J., Carvalho, B., Solorzano, R.D., Yang, M.T., Miller, J.S., Bhatia, S.N., and Chen, C.S. Geometric control of vascular networks to enhance engineered tissue integration and function. *Proc Natl Acad Sci U S A* **110**, 7586, 2013.
- Koffler, J., Kaufman-Francis, K., Shandalov, Y., Egozi, D., Pavlov, D.A., Landesberg, A., and Levenberg, S. Improved vascular organization enhances functional integration of engineered skeletal muscle grafts. *Proc Natl Acad Sci U S A* **108**, 14789, 2011.
- Chen, X., Aledia, A.S., Ghajar, C.M., Griffith, C.K., Putnam, A.J., Hughes, C.C., and George, S.C. Prevascularization of a fibrin-based tissue construct accelerates the formation of functional anastomosis with host vasculature. *Tissue Eng Part A* **15**, 1363, 2009.
- Chen, X., Aledia, A.S., Popson, S.A., Him, L., Hughes, C.C., and George, S.C. Rapid anastomosis of endothelial progenitor cell-derived vessels with host vasculature is

- promoted by a high density of cotransplanted fibroblasts. *Tissue Eng Part A* **16**, 585, 2010.
26. Sharma, A.K., Hota, P.V., Matoka, D.J., Fuller, N.J., Jandali, D., Thaker, H., Ameer, G.A., and Cheng, E.Y. Urinary bladder smooth muscle regeneration utilizing bone marrow derived mesenchymal stem cell seeded elastomeric poly(1,8-octanediol-co-citrate) based thin films. *Biomaterials* **31**, 6207, 2010.
  27. Sharma, A.K., Bury, M.I., Fuller, N.J., Rozkiewicz, D.I., Hota, P.V., Kollhoff, D.M., Webber, M.J., Tapaskar, N., Meisner, J.W., Lariviere, P.J., Destefano, S., Wang, D., Ameer, G.A., and Cheng, E.Y. Growth factor release from a chemically modified elastomeric poly(1,8-octanediol-co-citrate) thin film promotes angiogenesis in vivo. *J Biomed Mater Res A* **100**, 561, 2012.
  28. Sharma, A.K., Bury, M.I., Fuller, N.J., Marks, A.J., Kollhoff, D.M., Rao, M.V., Hota, P.V., Matoka, D.J., Edassery, S.L., Thaker, H., Sarwark, J.F., Janicki, J.A., Ameer, G.A., and Cheng, E.Y. Cotransplantation with

specific populations of spina bifida bone marrow stem/progenitor cells enhances urinary bladder regeneration. *Proc Natl Acad Sci U S A* **110**, 4003, 2013.

Address correspondence to:  
*Eric A. Kurzrock, MD*  
*Department of Urology*  
*University of California*  
*Davis School of Medicine*  
*4860 Y St., Suite 3500*  
*Sacramento, CA 95817*

*E-mail:* eric.kurzrock@ucdmc.ucdavis.edu

*Received: November 14, 2014*  
*Accepted: March 5, 2015*  
*Online Publication Date: April 22, 2015*